J Appl Electrochem (2009) 39:2535–2543
DOI 10.1007/s10800-009-9948-5

ORIGINAL PAPER

Inhibition of CO_2 corrosion of N80 carbon steel by carboxylic quaternary imidazoline and halide ions additives

P. C. Okafor · C. B. Liu · X. Liu · Y. G. Zheng

Received: 18 December 2008 / Accepted: 7 June 2009 / Published online: 18 June 2009

Abstract The inhibition of the corrosion of N80 mild steel by 2-undecyl-1-1-ethylamino-1-ethylcarboxyl quaternary imidazoline (CQI) in CO_2-saturated 3% NaCl and 3% Na_2SO_4 solutions was studied using electrochemical methods. Inhibition efficiency increased with increase in CQI concentration and synergistically increased in the presence of halide ions. CQI inhibited the corrosion reaction by chemical adsorption on the metal/solution interface in halide free solutions and by a combination of chemical and coulombic attraction in the presence of halide ions. The adsorption characteristics of the inhibitor were approximated by Frumkin isotherm and El-Awady et al. kinetic–thermodynamic model.

Keywords CO_2 corrosion · Mild steel · Imidazoline · Halide ions · Synergism

P. C. Okafor · C. B. Liu · X. Liu · Y. G. Zheng (✉)
State Key Laboratory for Corrosion and Protection,
Institute of Metal Research, Chinese Academy of Sciences,
62 Wencui Road, Shenyang, Liaoning Province 110016,
People's Republic of China
e-mail: ygzheng@imr.ac.cn; icpmkaist@yahoo.com

P. C. Okafor
Department of Pure and Applied Chemistry,
University of Calabar, P. M. B. 1115 Calabar, Nigeria
e-mail: pcokafor@chemist.com; pcokafor@gmail.com

X. Liu
Department of Applied Chemistry, Shenyang Institute
of Chemical Technology, Shenyang 110142,
People's Republic of China

1 Introduction

Aqueous CO_2 corrosion of carbon steel, which is an electrochemical process involving the anodic dissolution of iron and the cathodic evolution of hydrogen [1] has been widely acknowledged as a major factor in the degradation of oil and gas pipelines. It occurs principally in the form of general corrosion and three variants of localized corrosion (pitting, mesa attack and flow-induced localized corrosion) [2, 3] at all stages of production from downhole to surface equipment and processing facilities [4, 5]. At a given pH, CO_2 corrosion occurs at a much higher rate than would be found in a solution of a strong acid due to the presence of H_2CO_3 which enables hydrogen evolution at a much higher rate [1]. Due to the aggressiveness of CO_2-saturated solutions, inhibitors are usually used to minimize the corrosive attack on metallic materials and are reported to be the most cost effective and flexible means of corrosion control in the oil and gas production industry [5–8]. Of the numerous organic inhibitors used to combat CO_2 corrosion, imidazoline and its derivatives are reported to be among the most effective [5] and have been widely applied for the protection of CO_2 corrosion of oil and gas pipelines [7–15].

Imidazoline derivatives are an extensive group of nitrogen-based organic compounds that behave as cationic surfactants, depending on the nature of hydrocarbon or substituents groups attached to the carbon or nitrogen atoms of the imidazoline ring [16]. The inhibiting action of these compounds is attributed to their adsorption to the metal/solution interface [17]. Adsorption may occur via physisorption (involving electrostatic attraction between the charged metal and the charged inhibitor molecules) and/or via chemisorption (involving charge-sharing or charge-transfer from inhibitor molecules to the surface leading to the formation of coordinate-type bond [18]).

The latter may occur if the inhibitor contains lone pairs of electrons, multiple bonds or conjugated π-type bond system [18–22]. The adsorption process, and consequently the inhibition efficiency and even inhibition mechanism depend on the electronic and structural characteristics of the inhibitor, the nature of the surface, the temperature and pressure of the reaction [18], flow velocity as well as composition of the aggressive environment [23–25].

Synergistic inhibition, which is an improved performance of mixture of inhibitors compared with individual inhibitors [26] on the corrosion of metals, has proven to be an effective means of improving the inhibitive force of inhibitor, decreasing the amount of usage and to diversifying the application of inhibitor in acidic media [27]. On addition of halide ions to acid media containing any organic compound, a co-operative effect results which inhibits iron corrosion [27–30]. However halide ions either stimulate or inhibit the corrosion of metal, depending on their concentration [28, 29]. The inhibitive effects of halides have been reported to be in the order: $I^- \gg Br^- > Cl^-$ [28, 31]. The highest synergistic effect of iodide ions is reported to be due to chemisorption with metal surface due to its larger size and ease of polarizability [31]. More recently, and for the first time, the synergistic influence of iodide ions on CO_2 corrosion inhibition of mild steel by imidazoline derivative was reported [24].

In continuation of an extensive project carried out and still on-going in our laboratories to study the inhibitive properties of imidazoline derivatives in CO_2-saturated NaCl solutions under various experimental conditions, we present here a study of 2-undecyl-1-1-ethylamino-1-ethylcarboxyl quaternary imidazoline (CQI) with the molecular structure shown below:

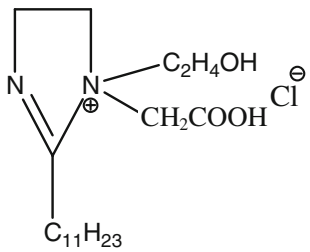

as corrosion inhibitor of N80 carbon steel in CO_2-saturated 3% NaCl and 3% Na_2SO_4 solutions as well as the effect of addition of iodide ions using electrochemical techniques.

2 Experimental

2.1 Materials preparation

N80 carbon steel cut from its parent pipe was used as the test material for these experiments and has the chemical composition shown in Table 1. The steel sheet was cut into coupons of dimension $1 \times 1 \times 0.8$ cm^3. The coupons were degreased with acetone in an ultrasonic water bath for about 10 min, air-dried, embedded in two-component epoxy resin and mounted in a PVC holder. A copper wire was soldered to the rear side of the coupon as an electrical connection. The exposed surface of the electrode (of area 1 cm^2) was wet-polished with silicon carbide abrasive paper up to 800 grits, rinsed with ethanol, placed in an ultrasonic acetone bath for about 5 min to remove possible residue of polishing and air-dried. This was used as the working electrode during the electrochemical test.

The test media were 3% NaCl and 3% Na_2SO_4. The latter was used to study the effects of the inhibitor and the synergistic effects of halide ions (Cl^- and I^-in CO_2-saturated halide free solutions. Before each test, the system was de-aerated by flushing with CO_2 gas for more than one hour and kept saturated with CO_2 by continuous flow of the gas at atmospheric pressure during the tests. The gas exit was sealed with distilled water. When needed, sodium hydrogen carbonate ($NaHCO_3$), was added to adjust the pH. For the 3% Na_2SO_4 solutions, diluted H_2SO_4 solution was used to lower the pH. The temperature was maintained within ± 1 °C in all experiments by placing the cell on a thermostated water bath. The pH was monitored with PB-10 Sartorius pH/temperature (°C) meter (with accuracy of ± 0.01) that was carefully calibrated with two buffer solution (pH 4 and 7). Electrochemical measurements were made using a PARSTAT® 2273 electrochemical measurement system connected to a computer and the results obtained were analysed using the circuits described in Okafor and Zheng [17].

The imidazoline used as inhibitor was synthesized, purified, characterized and supplied by one of the authors of the paper: X. Liu. No further treatments were carried out on them before use. Stock solution of the imidazoline (10,000 mg L^{-1}) was prepared with appropriate solvents and a micropipette was used to dispense the appropriate concentration into the corrosion cell. All chemicals used were of analar grade.

Table 1 Chemical composition of the N80 carbon steel

Element	C	Si	Mn	P	S	Al	Cu	Nb	Ni
Composition (wt%)	0.52	0.23	1.50	0.011	0.008	0.01	0.07	<0.005	0.02

2.2 Experimental procedure

Experiments were conducted in a three-electrode 500 mL glass cell setup with the counter electrode made of a platinum foil and the reference electrode being a saturated calomel electrode (SCE) connected to the cell externally through a Luggin capillary tube positioned close to the working electrode (N80 carbon steel) to minimize the ohmic potential drop.

The glass cell was filled with 350 mL of the test solution, de-aerated and saturated with carbon dioxide. The free corrosion potential was followed immediately after immersion until the potential stabilized within ±1 mV. The potentiodynamic polarization sweeps were conducted at a sweep rate of 0.2 mV s^{-1}. The solution and metal coupon were changed after each sweeps. In another set of experiments, LPR measurements were taken at ±5 mV around the corrosion potential by using a potentiodynamic scan at 0.1 mV s^{-1} followed by EIS measurements over the frequency range of 100 kHz to 10 mHz with a signal amplitude perturbation of 5 mV. All experiments were conducted at pH 4 to ascertain a uniform concentration of the corrosive carbonic species. For each experimental condition, two to three measurements were performed to estimate the repeatability. The repeatability was quite good, and the changes observed in the results reflect influences of various parameters beyond the experimental error.

3 Results and discussion

3.1 Inhibition by imidazoline (CQI)

3.1.1 Potentiodynamic polarization measurements

Potentiodynamic polarization curves were obtained to characterize the protection efficiency of CQI at a potential sweep rate of 0.2 mV s^{-1}. The polarization curves obtained for N80 mild steel in CO_2-saturated 3% NaCl solutions containing different concentrations of CQI at 25 °C are shown in Fig. 1. It is observed that the anodic and cathodic reactions were affected by the inhibitor. Based on this result, CQI is considered as a mixed-type inhibitor, which implies that, it reduces the anodic dissolution of the mild steel and also retards the cathodic reactions. Concerning the anodic region in relation to the zero current density potential, there is no evidence of passive film formation onto the electrode surface either in the presence or in the absence of the inhibitor. However, an anodic displacement of the corrosion potential (E_{corr}) and a decrease in the corrosion current density with increase in CQI concentration were also observed. This indicates the inhibiting effect of CQI on the mild steel corrosion which can be related to its adsorption on the steel surface blocking active sites.

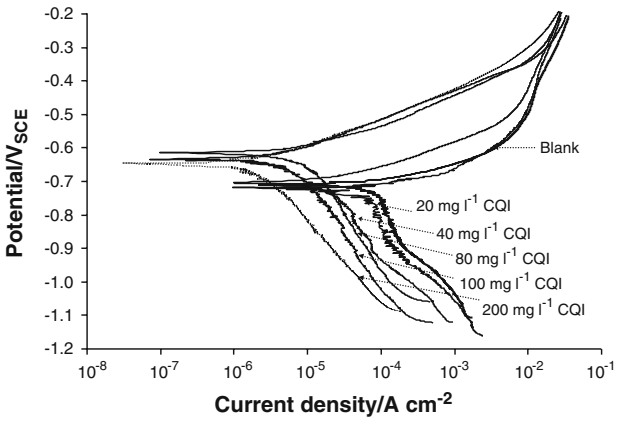

Fig. 1 Polarization curves for N80 mild steel in CO_2-saturated 3% NaCl solutions in the absence and presence of CQI at pH 4 and 25 °C

The values of the corrosion current density (i_{corr}) for N80 mild steel corrosion reaction in the absence and presence of the inhibitor were determined graphically by extrapolating the linear Tafel segment of the cathodic curves to the E_{corr} as described previously for non-Tafel dependence curves [17, 25, 32] and presented in Table 2. Also shown in Table 2 is the inhibition efficiency of CQI for the CO_2 corrosion of N80 mild steel calculated from the following equation:

$$\eta\% = \frac{i^0_{corr} - i_{corr}}{i^0_{corr}} \times 100 \quad (1)$$

where i^0_{corr} and i_{corr} are the uninhibited and inhibited corrosion current densities, respectively. It can be seen that CQI inhibits the CO_2 corrosion of N80 carbon steel to a large extent at all concentrations and temperatures studied and that the extent of inhibition is dependent on the inhibitor concentration. The inhibition efficiency increases with increasing inhibitor concentration.

The effect of temperature on the anodic and cathodic reactions in the absence and presence of 80 mg l^{-1} CQI for N80 carbon steel in 3% NaCl solutions saturated with CO_2 at pH 4 is represented in the polarization curves shown in Fig. 2. There is a clear acceleration of both the anodic and cathodic reactions with an increase in temperature. Similar curves have been reported previously [12]. The polarization parameters for the mild steel in the absence and presence of 80 mg l^{-1} CQI are listed in Table 2. It can be seen that the current density increased with temperature in the uninhibited and inhibited solutions. This is due to the acceleration of all the processes involved in corrosion: electrochemical, chemical, transport, etc. with increase in temperature [1]. It could also be noticed that increase in

Table 2 Polarization, EIS and LPR parameters for N80 mild steel in CO_2-saturated 3% NaCl solutions in the absence and presence of CQI CQI/iodide ions at 25 °C

Temperature (°C)	System	Polarization method			EIS method			LPR method	
		$-E_{corr}$ (V_{SCE})	I_{corr} (μA cm^{-2})	η%	R_{ct} (Ω cm^2)	$C_{dl} \times 10^{-4}$ (F cm^{-2})	η%	R_p (Ω cm^2)	η%
25	3% NaCl (blank)	713	96.4	–	168.9	2.1	–	167.3	–
	3% NaCl + 20 mg L^{-1} CQI	719	65.6	32.0	214.6	1.6	21.3	211.6	20.9
	3% NaCl + 40 mg L^{-1} CQI	703	21.0	78.3	931.0	0.7	81.9	803.1	79.2
	3% NaCl + 60 mg L^{-1} CQI	652	11.1	88.5	1620.4	0.7	89.6	939.9	82.2
	3% NaCl + 80 mg L^{-1} CQI	615	8.6	91.0	1927.6	0.6	91.2	1680.0	90.0
	3% NaCl + 100 mg L^{-1} CQI	633	6.1	93.7	2521.0	0.4	93.3	2270.0	92.6
	3% NaCl + 200 mg L^{-1} CQI	647	1.8	98.1	5379.9	0.6	96.9	5609.0	97.0
	3% NaCl + 80 mg L^{-1} CQI + 0.05 NaI	673	5.0	94.8	2206.0	1.4	92.3	2675.7	93.8
40	3% NaCl (blank)	714	182.0	–	102.6	2.1	–	89.6	–
	3% NaCl + 80 mg L^{-1} CQI	655	14.8	92.0	1316.0	0.6	92.2	1029	91.3

temperature increased the inhibition efficiencies of CQI suggesting chemisorption of the organic molecule on the surface of the metal. The apparent activation energies (E_a) for the corrosion of N80 mild steel in CO_2-saturated 3% NaCl solution in the absence and presence of the inhibitor were calculated from the condensed Arrhenius equation as follows:

$$\log \frac{i_{corr(2)}}{i_{corr(1)}} = \frac{E_a}{2.303R}\left(\frac{1}{T_1} - \frac{1}{T_2}\right) \quad (2)$$

where $i_{corr(1)}$ and $i_{corr(2)}$ are the corrosion current densities at temperatures T_1 (25 °C) and T_2 (40 °C), respectively. The calculated activation energy values in the absence and presence of the inhibitors are 32.8 and 27.8 kJ mol^{-1}, respectively. The decrease in activation energy in the presence of inhibitor is an indication of chemical adsorption of CQI on the surface of the metal [33]. This does not however, rule out possible contribution of electrostatic attraction to the corrosion inhibition process.

3.1.2 EIS and LPR measurements

Figure 3 shows representative of EIS measurements as Nyquist plots. The plot in the absence of inhibitor (inset) is characterized by a depressed semicircle from high to medium frequencies and an inductive loop at low frequencies. Similar curves for iron dissolution in acid solutions at E_{corr} have been reported previously [17, 24, 25, 34–36]. The appearance of the inductive loop observed in the Nyquist plots is attributed to the adsorption of an intermediate product in the corrosion reaction and the

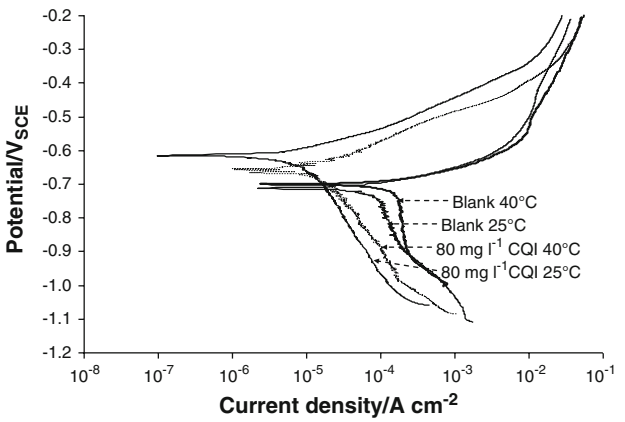

Fig. 2 Polarization curves for N80 mild steel in CO_2-saturated 3% NaCl solutions in the absence and presence of 80 mg L^{-1} CQI at pH 4 at 25 and 40 °C

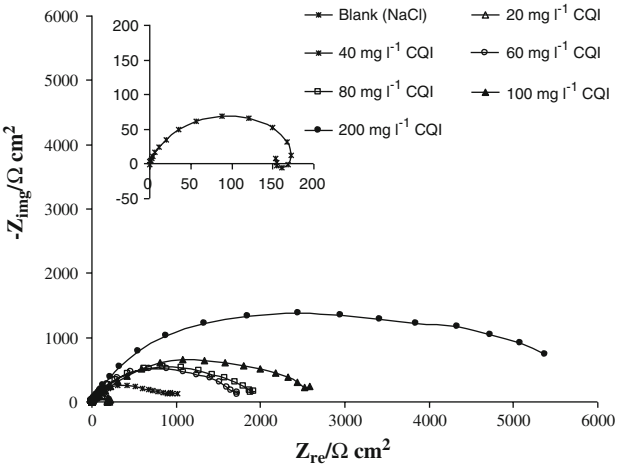

Fig. 3 Nyquist plots for N80 mild steel in CO_2-saturated 3% NaCl solutions in the absence (inset) and presence of CQI ions at pH 4 and 25 °C

capacitive semicircle is ascribed to the double layer capacitance and the charge transfer resistance of the corrosion process.

Introduction of the imidazoline was observed to increase the semicircle as shown in Fig. 3 indicating inhibition of the corrosion process and increase in CQI concentration increased the diameter of the semicircle. From the diameter of the single semicircle of the impedance diagram, the charge transfer resistance (R_{ct}) were determined. The values obtained in the absence and presence of inhibitors are as shown in Table 2. In the presence of CQI, the values of R_{ct} were observed to increase with increase in the concentration of CQI indicative of reduction in corrosion rate and consequently increase in the inhibiting ability of the imidazoline. It is also seen that the charge transfer resistance, R_{ct}, decreases with the increase in temperature.

The values of the capacitance for the semicircle (C_{dl}) were calculated from the equation:

$$C_{dl} = \frac{1}{2\pi f_{max} R_{ct}} \tag{3}$$

where f_{max} is the frequency corresponding to the maximum of the semicircle. The capacitance values were observed to decrease with the introduction of CQI. The decrease in C_{dl} values has been ascribed to a decrease in the dielectric constant and/or an increase in the double electric layer thickness, due to inhibitor adsorption on the metal/electrolyte interface [33, 37, 38]. This implies that the extent of adsorption on the metal/solution interface increases with CQI concentration.

Inhibition efficiency ($\eta\%$) is observed from Table 2 to increase with CQI concentration and followed the same trend as those obtained from the linear polarization resistance (in Table 2) measurements. The values were determined from the equation:

$$\eta\% = \frac{R_{ct(inh)} - R_{ct}}{R_{ct(inh)}} \times 100 \tag{4}$$

where R_{ct} and $R_{ct(inh)}$ are the uninhibited and inhibited charge transfer resistance, respectively. The inhibition efficiency values obtained for the three methods are in good agreement.

3.2 Adsorption isotherm

Figure 4 shows the adsorption curve for CQI on N80 mild steel in CO_2-saturated 3% NaCl solutions at 25 °C. The plot is characterized by an initial steeply rising part indicating the formation of a monolayer adsorbate film on the steel surface [38, 39] and as more inhibitor molecules become adsorbed at higher concentration, the adsorption rate is reduced. It is acknowledged that adsorption isotherms provide useful insights into the characteristics of the adsorption process and the mechanism of corrosion inhibition [40]. The experimental data obtained from the potentiodynamic polarization measurements were applied to different adsorption isotherm models. It was found that the data fitted the Frumkin adsorption isotherm (Fig. 5) and the El Awady et al kinetic–thermodynamic model (Fig. 6) which may be formulated, respectively as [18]:

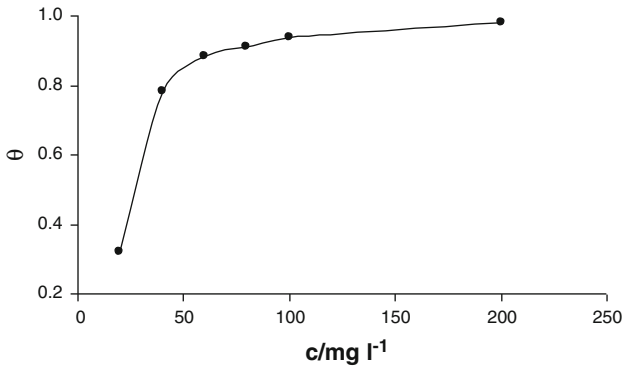

Fig. 4 Adsorption curve for CQI on N80 mild steel in CO_2-saturated 3% NaCl solutions at pH 4 and 25 °C

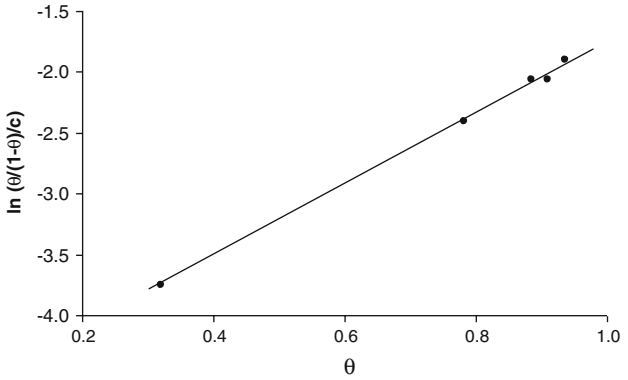

Fig. 5 Frumkin adsorption isotherm for CQI on N80 mild steel in CO_2-saturated 3% NaCl solutions at 25 °C

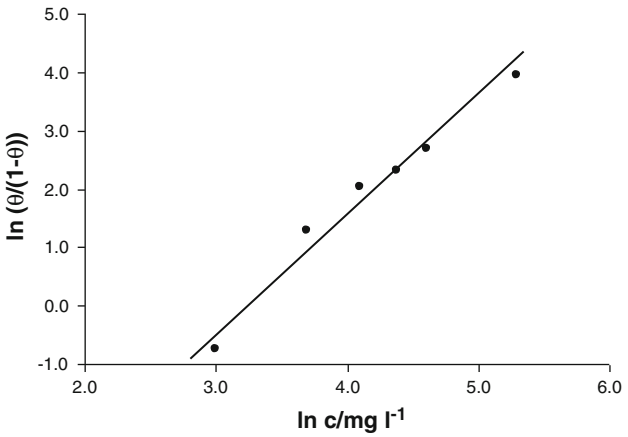

Fig. 6 El Awady kinetic–thermodynamic model for CQI on N80 mild steel in CO_2-saturated 3% NaCl solutions at 25 °C

$$\ln\left(\left(\frac{\theta}{1-\theta}\right)/c\right) = \ln K + 2a\theta \quad (5)$$

and

$$\log\left(\frac{\theta}{1-\theta}\right) = \log K' + y\log c \quad (6)$$

where θ is the degree of surface coverage ($\theta = \eta\%/100$), a is an interaction parameter, y is the occupancy parameter, the inverse ($1/y$) of which gives the size parameter and a measure of the number of adsorbed water molecules substituted by a given inhibitor, K is the equilibrium (or binding) constant of the adsorption reaction and $K = K'^{(1/y)}$. The adsorption parameters deduced from the isotherms are presented in Table 3. The molecular interaction parameter can have both positive and negative values. Positive values of a indicate attraction forces between adsorbed molecules while negative values indicate repulsive forces between the adsorbed molecules [41]. It is seen in the table that positive value of a was obtained indicating that attraction exists in the adsorption layer. Positive values of a have also been interpreted to imply that the interactions between molecules cause an increase in the adsorption energy with the increase of surface coverage [18, 42]. The size parameter value (0.5) obtained indicates the formation of multilayers of the inhibitor on the surface of the metal [18]. This is made possible due to the attraction between the molecules (as indicated by the positive values of the interaction parameter) which may make it less difficult for more molecules to get adsorbed on a neighbouring site. The k_{ad} values denote the strength between the adsorbate and adsorbent. Large values of K imply more efficient adsorption.

The constant, K, is related to the standard free energy of adsorption ΔG^0_{ads} by the equation:

$$K = \frac{1}{55.5}\exp\left(\frac{-\Delta G^0_{ads}}{RT}\right) \quad (7)$$

The value of 55.5 being the concentration of water in solution expressed in mole. The calculated values from the different isotherms are shown in Table 3. The negative value indicates a spontaneous adsorption of CQI on the surface of the metal and confirms the proposed chemical adsorption mechanism. Generally, values of ΔG^0_{ads}more negative than -40 kJ mol^{-1} involve charge-sharing or transfer from the inhibitor molecules to the metal surface to form a coordinate type of bond indicating chemical adsorption [43–45].

Table 3 Kinetic and thermodynamic parameters for the adsorption of CQI on N80 mild steel in CO_2-saturated 3% NaCl solutions at 25 °C

Thermodynamic–kinetic model			Frumkin isotherm		
a	ln K	$-\Delta G$ (kJ mol^{-1})	$1/y$	ln K'	$-\Delta G$ (kJ mol^{-1})
1.4	8.0	79.6	0.5	9.5	94.1

3.3 Effects of halide ions

In order to access the effect of halide ions on the CO_2 corrosion in the absence and presence of imidazolines, potentiodynamic polarization, linear polarization resistance (LPR) and electrochemical impedance spectroscopic (EIS) measurements were carried out in CO_2-saturated 3% Na_2SO_4 solutions with and without 0.05 M Cl^-, 0.05 M I^-, 80 mg l^{-1} CQI and 0.05 M Cl^-/80 mg l^{-1} CQI and 0.05 M I^-/80 mg l^{-1} CQI mixtures. Na_2SO_4 solution was used to remove any interference from the chloride ion in NaCl solution so that the effects of the halide ions would be clearly appreciated. The results obtained from these measurements are shown in Figs. 7, 8 and Table 4.

Figure 7 shows the polarization curves for N80 mild steel in CO_2-saturated 3% Na_2SO_4 solutions in the absence and presence of CQI and CQI/halide ions mixture at 25 °C. The polarization parameters deduced from the curves are shown in Table 4. It is observed that addition of CQI and CQI/halide ions mixtures reduced the rates of the anodic and cathodic reactions as evident in the reduction in the current densities, and positively shift the corrosion potential. The extent of inhibition is found to be in the order: CQI/I^- > CQI/Cl^- > CQI. Addition of halide ions to acidic solutions containing organic compounds is generally accepted to synergistically increase the inhibition efficiency by forming intermediate bridges between the negatively charged surface and the positively charge organic compound. The greater synergistic effects of iodine ions compared to chloride ions is attributed to its large ionic size, hydrophobicity and ease of polarizability which facilitates electron pair bonding with the iron surface

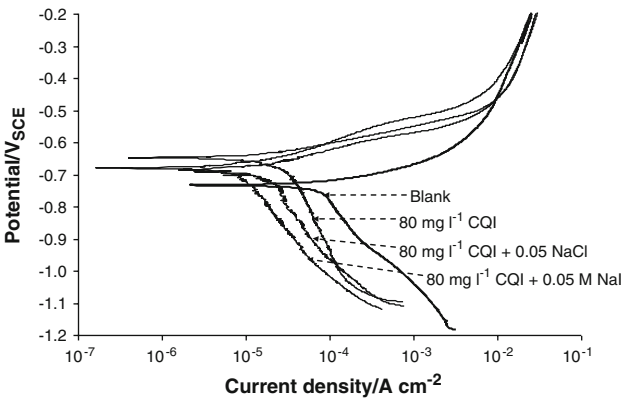

Fig. 7 Polarization curves for N80 mild steel in CO_2-saturated 3% Na_2SO_4 solutions in the absence and presence of 80 mg L^{-1} CQI and CQI/halide ions at pH 4 at 25 °C

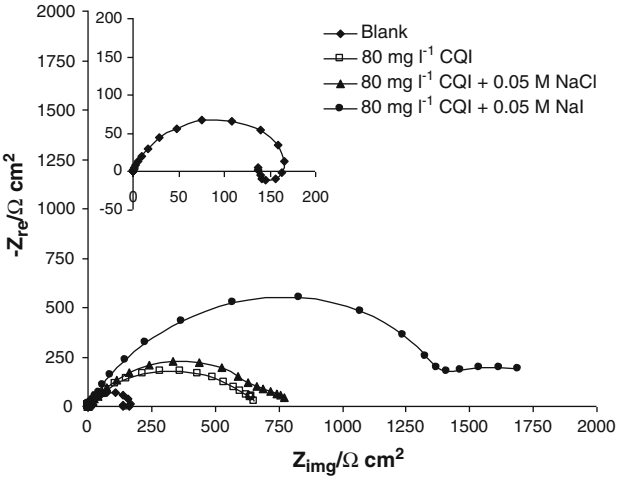

Fig. 8 Nyquist plots for N80 mild steel in CO_2-saturated 3% Na_2SO_4 solutions in the absence and presence of 80 mg L^{-1} CQI and CQI/halide ions at pH 4 at 25 °C

[31, 46, 47]. Comparing the values of I_{corr} and $\eta\%$ (in Tables 2 and 4) for N80 mild steel in CO_2-saturated 3% Na_2SO_4 solutions containing CQI/I^- with those obtained in 3% NaCl, it could be observed that in NaCl solution, the mixture exhibited a more inhibiting ability. This could be ascribed to synergistic effect as a result of the presence of both Cl^- and I^- in the system.

Figure 8 shows the impedance behaviour of N80 mild steel in CO_2-saturated 3% Na_2SO_4 solutions in the absence and presence of CQI and CQI/halide ions mixture at 25 °C. The results obtained from these curves are summarized in Table 4. In the absence of inhibitors the plots are characterized by a depressed semicircle from high to medium frequencies and an inductive loop at low frequencies similar to that in 3% NaCl solution. This signifies that the corrosion mechanism did not change with change in electrolyte. The appearance of the inductive loop and the capacitive semicircle is attributed to the adsorption of an intermediate product in the corrosion reaction and the double layer capacitance/transfer resistance, respectively. The same characteristic high frequency impedance behaviour of the N80 mild steel in CO_2-saturated 3% Na_2SO_4 solutions was observed on introduction of halide ions. However, a slight decrease in charge transfer resistance (from 153.6 to 151.8 Ω cm^2) in the presence of Cl^- indicating acceleration of the corrosion process and an increase (from 153.6 to 236.4 Ω cm^2) in the presence of I^- indicating inhibition of the corrosion process was observed.

Introduction of 80 mg l^{-1} CQI into the corrodent leads to an increase in the charge transfer resistance from 153.6 to 664.1 Ω cm^2 resulting in 76.9% of inhibition efficiency and a decrease in the double layer capacitance C_{dl} from 2.29×10^{-4} to 9.2×10^{-5} F cm^{-2}. The decrease in C_{dl} values has been ascribed to a decrease in the dielectric constant and/or an increase in the double electric layer thickness, due to inhibitor adsorption on the metal/electrolyte interface [33, 37, 38]. Introduction of 0.05 M of halide ions into the system containing 80 mg l^{-1} CQI resulted in further increase in charge transfer resistance and inhibition efficiencies indicating synergism, and decrease in C_{dl} values. The order of increase in inhibition efficiencies is CQI/$I^- \gg$ CQI/Cl^- > CQI. From Fig. 8 it could be observed that the impedance diagrams for N80 mild steel in the presence of 80 mg l^{-1} CQI + 0.05 M NaI is characterized by high frequency capacitive and an indications of low frequency capacitive loops. Similar curves have been reported previously for iron dissolution in acid medium in the presence of high concentration of halide ion [17]. The existence of the capacitive loops and disappearance of the low frequency inductive loops compared with the Nyquist diagram in the absence of inhibitor could be related to the gradual replacement of water molecules and/or hydroxyl ions by iodide ions on the surface of the metal and consequently reducing the active sites necessary for the coupled dissolution reaction, involving hydroxyl ions as proposed by Barcia and Mattos [48] for iron in acid media.

Table 4 Polarization, EIS and LPR parameters for N80 mild steel in CO_2-saturated 3% Na_2SO_4 solutions in the absence and presence of CQI, halides and CQI/halide mixture at 25 °C

System	Polarization method			EIS method			LPR method	
	$-E_{corr}$ (V_{SCE})	I_{corr} (μA cm^{-2})	$\eta\%$	R_{ct} (Ω cm^2)	$C_{dl} \times 10^{-4}$ (F cm^{-2})	$\eta\%$	R_p (Ω cm^2)	$\eta\%$
3% Na_2SO_4 (blank)	733	76.4	–	153.6	2.29	–	156.2	–
3% Na_2SO_4 + 0.05 M NaCl	735	74.7	2.2	151.8	2.32	−1.2	155.7	−0.3
3% Na_2SO_4 + 0.05 M NaI	734	61.0	20.1	236.4	2.60	35.0	220.1	29.0
3% Na_2SO_4 + 80 mg L^{-1} CQI	647	26.2	65.7	664.1	0.92	76.9	629.3	75.2
3% Na_2SO_4 + 80 mg L^{-1} CQI + 0.05 M NaCl	688	16.7	78.1	843.2	0.73	81.8	802.9	80.6
3% Na_2SO_4 + 80 mg L^{-1} CQI + 0.05 M NaI	679	7.2	90.6	1487.0	0.72	89.7	1651.8	90.6

Similar view is also held by Bartos and Hackerman [49] for iron in hydrochloric acid.

From the linear polarization resistance (LPR) studies, polarization resistance values (Table 4) followed the same trend as the charge transfer resistance values for the systems studied and the inhibition efficiencies obtained from both methods are in good agreement.

3.4 Mechanism of corrosion inhibition

Inhibition of mild steel corrosion in CO_2-saturated solutions by imidazoline derivatives can be explained on the basis of adsorption. The adsorption of organic compounds can be described by two main types of interaction: physisorption and chemisorption. In the former, the presence of electrically charged metal surface and charged species in the bulk of the solution is required, while the latter (chemisorption) involves charge-sharing or charge-transfer from the inhibitor molecules to the metal surface to form a coordinate type of a bond. This is possible in case of a positive as well as a negative charge on the surface [27]. It is worth noting that a combination of both processes is possible [50]. The molecular structure of CQI is composed of a five-member ring containing nitrogen elements (the head group), a C-11 saturated hydrophobic group and a hydrophilic ethylcarboxylic group attached to the N1 atom. Also attached to the N1 atom is a quaternary ethylcarboxylic group that gives the compound a positive charge. The compound can be adsorbed on the metal surface by the formation of an iron-nitrogen co-ordination bond and by a pi-electron interaction between the pi-electron in the head group and iron. The adsorption of CQI on the steel surface creates a barrier for mass and charge transfers. Comparing the inhibition efficiencies of the compound in both studied media (3% NaCl and 3% Na_2SO_4 solutions), it was observed that the imidazoline exhibited a higher efficiency in the 3% NaCl than in the Na_2SO_4 solutions. It is reported that the surface of iron is found to be positively charged in an inhibitor-free sulphate containing solution [51] and the protonated inhibitor compound species would be less strongly adsorbed onto the metal surface resulting in less inhibition efficiencies [31]. In the presence of halide ions, the surface of the metal is negatively charged (as a result of the specific adsorption of chloride ions) and coulombic attraction between the metal and the imidazoline contributes to the higher inhibition efficiency observed in the NaCl solutions.

4 Conclusions

2-undecyl-1,1-dicarboxylethyl quaternary imidazoline (CQI) is found to inhibit the corrosion of mild steel in CO_2-saturated 3% NaCl and 3% Na_2SO_4 solutions and the extent of inhibition is dependent on CQI concentration and on temperature. A mixed-inhibition mechanism is proposed for the inhibitive effects of CQI. The values of the corrosion activation energy in the absence and presence of CQI in CO_2-saturated 3% NaCl and Gibbs free energy of adsorption indicates that CQI is chemically adsorbed on the surface of the metal. CQI inhibited the corrosion reaction by chemical adsorption on the metal/solution interface in halide free solutions and by a combination of chemical and coulombic attraction in the presence of halide ions. The adsorption characteristics of the inhibitor were approximated by Frumkin isotherm and El-Awady et al. kinetic–thermodynamic model. Inhibition efficiency of CQI was enhanced by the addition of halide ions due to synergistic effects. The order of synergism is found to be $I^- > Cl^-$.

Acknowledgement PCO acknowledges the Chinese Academy of Sciences (CAS) and the Academy of Sciences for the Developing World (TWAS) for the CAS-TWAS Postdoctoral Fellowship.

References

1. Nesic S (2007) Corros Sci 49:4308
2. Kermani MB, Smith LM (eds) (1994) Predicting CO_2 corrosion in oil and gas industry. European Federation of Corrosion Publication number 13. Institute of Materials, London
3. Kermani MB, Morshed A (2003) Corrosion 59:659
4. Fu SL, Garcia JG, Griffin AM (1996) In: Proceedings of CORROSION/1996, Paper no. 21, NACE International, Houston
5. Durnie W, Kinsella B, De Marco R, Jefferson A (2001) J Appl Electrochem 31:1221
6. Webster S, Harrop D, McMahon A, Partidge GJ (1993) In: Proceedings of CORROSION/1993, Paper no. 109, NACE International, Houston
7. Tan YJ, Bailey S, Kinsella B (1996) Corros Sci 38:1545
8. Ramachandran S, Jovancicevic V (1999) Corrosion 55:259
9. Hong T, Sun YH, Jepson WP (2002) Corros Sci 44:101
10. Bilkova K, Hackerman N (2002) In: Proceedings of CORROSION/2002, Paper no. 284, NACE International, Houston
11. Lopez DA, Schreiner WH, de Sanchez SR, Simison SN (2003) Appl Surf Sci 207:69
12. Zhang G, Chena C, Lub M, Chai C, Wu Y (2007) Mater Chem Phys 105:331
13. Liu X, Zheng YG (2008) Corros Eng Sci Tech 43:87
14. Xia S, Qiu M, Yu L, Liu F, Zhao H (2008) Corros Sci 50:2021
15. Paolinelli LD, Pérez T, Simison SN (2008) Corros Sci 50:2456
16. Cruz J, Martínez-Aguilera LMR, Salcedo R, Castro M (2001) Inter J Quantum Chem 85:546
17. Okafor PC, Zheng YG (2009) Corros Sci 51:850
18. El-Awady AA, Abd-El-Nabey BA, Aziz SG (1992) J Electrochem Soc 139:2149
19. Hackerman N (1962) Corrosion 18:322
20. Ateya B (1972) J Electroanal Chem 76:91
21. Nobe K, Eldakar N (1981) Corrosion 37:271
22. Ebenso EE, Ekpe UJ, Ita BI, Offiong OE, Ibok UJ (1999) Mater Chem Phys 60:79
23. Jiang X, Zheng YG, Ke W (2005) Corros Sci 47:2636
24. Okafor PC, Liu X, Zheng YG (2009) Corros Sci 51:761
25. Liu X, Okafor PC, Zheng YG (2009) Corros Sci 51:744

26. Ekpe UJ, Okafor PC, Ebenso EE, Offiong OE, Ita BI (2001) Bull Electrochem 17:131
27. Abdel Rehim SS, Hazzazi OA, Amin MA, Khaled FK (2008) Corros Sci 50:2258
28. Okafor PC, Oguzie EE, Iniama GE, Ikpi ME, Ekpe UJ (2008) Glob J Pure Appl Sci 14:89
29. Ebenso EE, Okafor PC, Ibok UJ, Ekpe UJ, Onuchukwu AI (2004) J Chem Soc Niger 29:15
30. Umoren SA, Ebenso EE, Okafor PC, Ekpe UJ, Ogbobe O (2006) J Appl Polym Sci 103:2810
31. Jeyaprabha C, Sathiyanarayanan S, Venkatachari G (2006) Electrochim Acta 51:4080
32. Reznik VS, Akamsin VD, Khodyrev YP, Galiakberov RM, Efremov YY, Tiwari L (2008) Corros Sci 50:392
33. Popova A, Sokolova E, Raicheva S, Christov M (2003) Corros Sci 45:33
34. Keddam M, Mattos OR, Takenouti H (1981) J Electrochem Soc 128:257
35. Lorenz WJ, Mansfeld F (1981) Corros Sci 21:647
36. Okafor PC, Brown B, Nesic S (2008) CO_2 corrosion of carbon steel in the presence of acetic acid at higher temperatures. J Appl Electrochem. doi: 10.1007/s10800-008-9733-x
37. Sayed SY, El-Deab MS, El-Deab BE, El-Anadouli BE, Ateya BG (2003) J Phys Chem B 107:5575
38. Oguzie EE, Li Y, Wang FG (2007) J Colloid Interface Sci 310:90
39. Ameer MA, Khamis E, Al-Senani G (2000) Ads Sci Tech 18:177
40. Durnie W, De Marco R, Jefferson A, Kinsella B (1999) J Electrochem Soc 146:1751
41. Noor EA (2007) Int J Electrochem Sci 2:996
42. Szklarska-Smialowska Z, Wieczorek G (1970) In: Proceedings of the 3rd European symposium on corrosion inhibitors. Ann Univ Ferrara, N. S. Sez V, Suppl. No. 5
43. Shize D, Yiling T (eds) (1990) Interface chemistry. High Grade Education Press, Beijing
44. Bilgic S, Sahin M (2001) Mater Chem Phys 70:290
45. Okafor PC, Ebenso EE, Ekpe UJ, Ibok UJ, Ikpi ME (2003) Trans SAEST 38:91
46. Hackerman N, Snavely ES, Paayne JS (1966) J Electrochem Soc 113:677
47. Kuznetsov YI, Andreev NN (1996) In: Proceedings of CORROSION/1996, Paper no. 214, NACE International, Houston
48. Barcia OE, Mattos OR (1990) Electrochim Acta 35:1601
49. Bartos M, Hackerman N (1992) J Electrochem Soc 139:3428
50. Mansfeld F (1987) Corrosion mechanisms. Mercel Dekker Inc, New York
51. Murakawa T, Hackerman N (1964) Corros Sci 4:357